Testing the limit of AO for ELTs: diffraction limited astronomy in the red optical

M. Tecza[a], J. Magorrian, N. Thatte, and F. Clarke

University of Oxford, Department of Physics, Denys Wilkinson Building, Oxford, OX1 3RH, United Kingdom

Abstract. Many of the proposed science cases for extremely large telescopes (ELT) are only possible because of the unprecedented sensitivity and spatial resolution due to advanced, e.g. tomographic and multi conjugate, adaptive optic (AO) systems. Current AO systems on 8-10 m telescopes work best at wavelengths longward of 1 μm with Strehl ratios $\geq$ 15%. At red-optical wavelengths, e.g. in the I band (0.8 μm), the Strehl ratio is at best a few percent. The AO point spread function (PSF) typically has a diffraction-limited core superimposed on the seeing halo, however, for a 5% Strehl ratio the core has a very low intensity above the seeing halo. At an ELT, due to a 3-4 times higher angular resolution, the diffraction limited PSF core of only 5% Strehl ratio stands more prominently atop the shallow seeing halo leading to almost diffraction limited image quality even at low Strehl ratios. Prominent ELT science cases that use the Calcium triplet can exploit this gain in spatial resolution in the red-optical: stellar populations in dense environments or crowded fields; and the case of intermediate mass black holes in nuclear and globular stellar clusters, as well as (super-) massive black holes in galaxies.

1 The power of Extremely Large Telescopes

The advent of Extremely Large Telescopes (ELT) will open a new parameter space of unprecedented spatial resolution and sensitivity. Historically, telescope diameters approximately doubled from one generation to the next, however, the future ELTs will break this trend and have diameters that are about 3 to 4 times larger than the biggest optical telescopes in operation today.

[a] m.tecza@physics.ox.ac.uk

1.1 Increased angluar resolution

With the increase in telescope diameter D naturally comes a much smaller diffraction limited angular resolution $\theta_{BH} \approx \lambda/D$. To reach this resolution, ELTs must be equipped with advanced adaptive optics (AO) systems for the real-time compensation of atmospheric turbulence and windshake effects. For example the 40 m European ELT (E-ELT) will achieve $\approx$ 8 mas angular resolution when combined with the laser tomographic AO (LTAO) system ATLAS [1] (see Figure 1). At a redshift z$\approx$1 this angular resolution will allow an ELT to resolve structures of a few tens of parsecs in size, the approximate size of a major star-forming region.

1.2 Increased sensitivity

The other obvious advantage of an ELT is its enormous light collecting power. For a fixed angular resolution the time necessary to reach a certain signal-to-noise ratio (SNR) scales as $1/D^2$. An ELT therefore is more than one magnitude faster compared to the largest optical telescopes. However, the biggest gain is achieved when combining the increased angular resolution with the increased collecting area of an ELT. As the linear image size of a point source is proportional to λ/D, and its area therefore proportional to $(\lambda/D)^2$, the time to reach the same SNR of a point source scales as $1/D^4$, a factor 100-200 times faster than possible today.

1.3 Science with Extremely Large Telescopes

All aspects of astronomy, from studies of our own Solar System to the furthest observable objects at the edge of the visible Universe, will benefit from the enormous improvements in collecting area and angular resolution. Among the key science cases for an ELT are the direct imaging of extra-solar planets or even earths, which is only made possible because of the increased angular resolution of an ELT. The increased collecting area of an ELT will allow us to survey and spectroscopically identify for the first time the most distant high redshift galaxies, and detect sources responsible for the first light during the epoch of re-ionisation.

Another principle science case of an ELT is to study the resolved stellar populations of galaxies spanning the full range of morphologies, the ultimate goal being to reach the rich and diverse galaxy population of the Virgo cluster.

To make direct measurements of the chemo-dynamical properties of resolved stars we need accurate velocity measurements combined with metallicity indicators for a significant number ($\approx$1000) of stars in the galaxy's sub-components, e.g. the thin and thick disc, the halo, and the bulge. Traditionally medium resolution spectroscopy (R$\approx$4,000-10,000) of the Ca triplet at 0.85 μm is used to yield the velocity and metallicity measurements simultaneously. To obtain the spectra of many stars at the same time AO assisted integral field spectroscopy is a very efficient tool.

However, the major limiting factor of these studies, apart from sensitivity, is crowding. Especially for the brighter galaxies, observations will be limited to the less representative outer regions. If it is possible to achieve almost diffraction limited image quality at 0.85 μm these studies could be pushed into the more interesting, denser regions of galaxies.

2 AO assisted integral field spectroscopy in the red-optical

Especially the case of resolved stellar population described in §1.3 demonstrates the need for high angular resolution and hence for advanced AO systems that can achieve reasonable Strehl ratios at red-optical wavelengths.

2.1 Increased angular resolution and sensitivity

Typically an AO point spread function (PSF) consists of a seeing halo on top of which a much narrower diffraction-limited core is superimposed. Current AO systems at 8-10 m telescopes deliver I band PSFs with Strehl ratios of a few percent at best, with little flux in the diffraction limited core that is approximately 30 times narrower than the seeing halo.

At an ELT however, the same flux is concentrated into a diffraction-limited core that is 3-4 times narrower, leading to a PSF with increased PSF peak intensity and discernable diffraction limited core (see Figure 1).

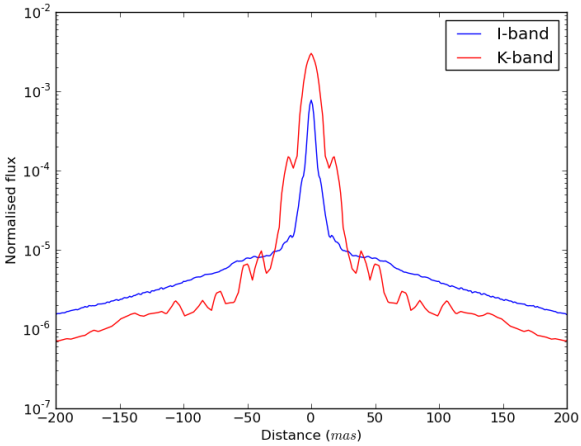

Fig. 1. E-ELT LTAO: I and K band PSF cross-section (data courtesy T. Fusco).

This promises almost diffraction limited resolution in the red-optical even if the Strehl ratio is only a few percent ([2], Figure 2). In addition to the possible high angular resolution observing in the I band offers the advantage of a much reduced sky-background which can increase the sensitivity by a factor of 2-3 (see Figure 2).

2.2 HARMONI

For the E-ELT the first-light spectrograph will be an AO assisted optical and near-infrared integral field spectrograph. The instrument will be based on the HARMONI [3] design developed as one of the E-ELT's Phase A instrument studies in 2008-2010. HARMONI covers a wavelength range from 0.47-2.45 μm at resolving powers of R ($\equiv \lambda/\Delta\lambda$)$\approx$4000, 10000, and 20000. It has a field-of-view (FoV) of 256×128 spaxel with selectable angular sizes of 4, 10, 20, and 40 mas. HARMONI is designed to be a workhorse instrument for the E-ELT enabling a wide range of science to be carried in the early days of the telescope.

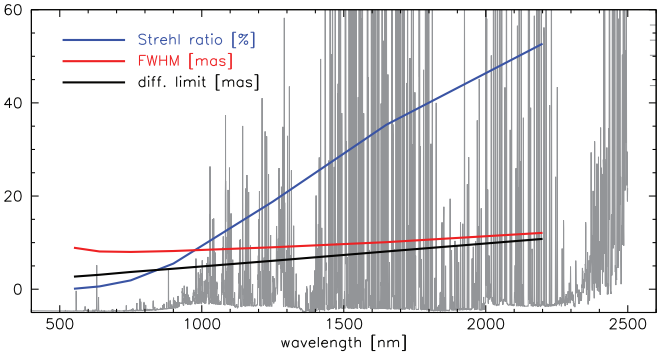

Fig. 2. E-ELT LTAO: FWHM (red), Strehl ratio (blue) and diffraction limited FWHM (black) over-plotted on the sky-background spectrum (grey).

3 Black holes with HARMONI

Among the many science cases that HARMONI will address (see [3], [4]) a few will benefit more from near diffraction limited angular resolution in the I band. In this chapter we present the selected case of black holes, in particular super-massive black holes and inter-mediate mass black holes.

3.1 Super-massive Black Holes

Many, and perhaps all, luminous galaxies contain super-massive black holes in their centres. These nuclear black holes are a basic component of galaxies. Stellar and gas dynamical studies over the last decade have demonstrated the existence of a tight correlation between the stellar velocity dispersion of the bulges and the mass of the black hole in luminous galaxies [5]. Recent studies of early-type galaxies in the Virgo cluster [6] indicate that bright massive ($M > \text{few } 10^{10}\,M_{\odot}$) galaxies would often, or perhaps always, contain massive black holes but not stellar nuclei. In less massive galaxies, stellar nuclei would become common with massive black holes even disappearing at the low mass end. If true, this has important implications for the physical scenarios of galaxy formation.

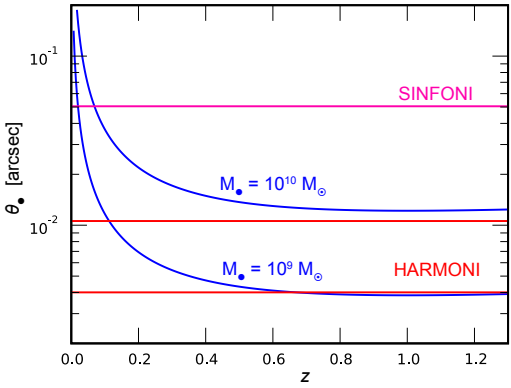

Fig. 3. Black hole sphere of influence as a function of redshift for two different black hole masses: 10^9 $M_\odot$) and 10^{10} $M_\odot$. The spatial resolution of SINFONI of 50 mas and HARMONI at 11 and 4 mas are shown as horizontal lines.

The mass of the central black hole in most galaxies can only be measured reliably through the gravitational effect on the gas and/or stars within its sphere of influence $\theta_{BH} = G \cdot M_{BH}/\sigma^2$, i.e. the region where the gravitational influence of the black hole dominates that of the surrounding stars. For super-massive black holes in nearby galaxies the sphere of influence is typically of the order of few to several parsecs.

In Figure 3 we show the sphere of influence for two black hole masses, 10^9 $M_\odot$ and 10^{10} $M_\odot$), as a function of redshift. For example SINFONI [7] working at the diffraction limit of the Very Large Telescope has an angular resolution of ≈50 mas in the K band and can detect a 10^9 $M_\odot$ black hole out to a distance of ≈20 Mpc. HARMONI at the E-ELT achieves a K band angular resolution of 11 mas and will detect a 10^9 $M_\odot$ black hole out to a distance of ≈100 Mpc and a 10^{10} $M_\odot$ black hole at any redshift.

To measure the mass of the black hole one determines a map of the line-of-sight velocity distributions (LOSVD) from stellar absorption features like the CO band-head at 2.3 μm and fits to it a model of the two-dimensional stellar kinematics with the black hole mass as a free parameter. In the I band using the Ca triplet at 0.85 μm HARMONI could in

principle reach a spatial resolution of ≈4 mas and therefore will be able to detect even a 10^9 $M_\odot$) black hole at any redshift.

3.2 Intermediate mass black holes in nuclear stellar clusters

There are many reasons to expect that black holes might exist with masses in the range 10^2 to 10^5 $M_\odot$, intermediate between stellar-mass and supermassive black holes. Such intermediate-mass black holes (IMBH) could plausibly form as a natural result of the evolution of dense star clusters, or in the same (as yet unknown) process that produces supermassive black holes. Alternatively, they could be remnants of the first generation of stars.

There is no unambiguous observational evidence that they exist, however. The natural places to look for IMBHs are in the centres of Galactic globular clusters and the nuclear stellar clusters (NSC) found at the centres of most late-type galaxies. In NSCs one cannot resolve individual stars and so must adopt integrated light methods similar to those used for finding SMBHs in external galaxies.

To test the feasibility of detecting an IMBH within an NSC with HARMONI, we constructed a simulated NSC based on IC 342 [8]. Our simulated NSC has a spherical King density function with a half-mass radius of 2.9 pc, to which we add black holes with masses of $1.4 \cdot 10^5$ $M_\odot$, $3 \cdot 10^5$ $M_\odot$, and $5 \cdot 10^5$ $M_\odot$. The mean luminosity-weighted velocity dispersion has been scaled to $\approx$ 36 $km\,s^{-1}$ resulting in a total cluster mass of $\approx$ 10^6 $M_\odot$. The results of our simulations are shown in Figure 4 where we show both the velocity dispersion σ and the Gauss-Hermite polynomial coefficient h_4 as a function of radial separation from the cluster centre. One can see that the NSC with a $3 \cdot 10^5$ $M_\odot$ black hole can easily distinguished from the NSC model without black hole.

Having shown that HARMONI is in principle able to detect IMBHs in NSCs, we next investigated whether the E-ELT LTAO PSF would limit our experiment. As in the case of the SMBHs we concentrated on the K and I bands as they cover the prominent stellar absorption features of CO and Ca, respectively. We present our results in Figure 5. As can be seen neither the velocity dispersion nor the Gauss-Hermite coefficient h4 are very much affected by the K band PSF, however the I band PSF noticeable smears both parameters. Nevertheless, it is still possible to distinguish between an NSC without a black hole and an NSC with a $3 \cdot 10^5$ $M_\odot$ black hole.

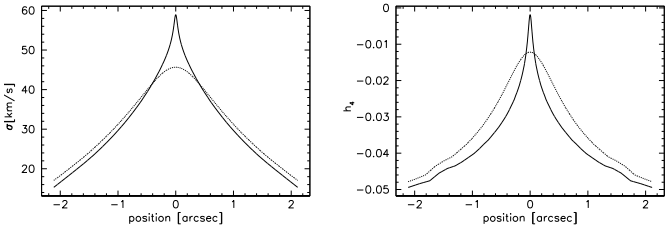

Fig. 4. Velocity dispersion (right) and Gauss-Hermite coefficient h_4 of our NSC as a function of radial separation. Dashed lines: NSC without black hole. Solid lines: NSC with a black hole of mass $3 \cdot 10^5$ $M_\odot$.

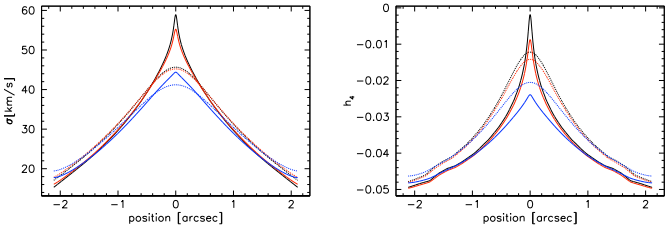

Fig. 5. Velocity dispersion (left) and Gauss-Hermite coefficient h4 (right) of our NSC as a function of radial separation after convolution with the K band (red) and I band (blue) ATLAS-LTAO point spread function. Dashed lines: NSC without black hole. Solid lines: NSC with a black hole of mass $3 \cdot 10^5$ $M_\odot$.

References

1. T. Fusco, et al., This conference, (2011)
2. T. Fusco, The Messenger, **140**, pp. 18 (2011)
3. N. Thatte, et al., SPIE, **7735**, pp. 85 (2010)
4. N. Thatte, The Messenger, **140**, pp. 26 (2010)
5. L. Ferrarese & H. Ford, Space Science Review, **116**, 523 (2005)
6. L. Ferrarese et al., ApJ, **644**, L21 (2006)
7. F. Eisenhauer et al., SPIE, **4841**, pp. 1548 (2003)
8. T. Böker et al., AJ, **118**, 2, pp. 831 (1999)